Int. J. Solids Structures, 1970, Vol. 6, pp. 1243 to 1258. Pergamon Press. Printed in Great Britain

CHANGES OF WAVE-FORM OF PLATES IN THE POST-BUCKLING RANGE

W. J. SUPPLE

Department of Engineering Science, Oxford University

Abstract—The post-buckling behaviour of thin rectangular plates in axial compression is considered. The plates are considered as having two degrees of freedom characterized by buckling in m and n halfsinewaves axially and uncoupled and coupled buckling modes are established for specified boundary conditions. The results of the investigation together with results for different boundary conditions from other sources are used to explain abrupt changes in waveform of plates in the post-buckling range. The effects of initial geometric imperfections are included as a necessary part of the analysis.

1. INTRODUCTION

THE post-buckling behaviour of thin plates is an important topic in structural mechanics since plates are possibly unique in their extensive use as load-carrying structural components up to and into the post-buckling range. The axial stiffness of a plate after buckling is approximately one half of the pre-buckled value, the exact value being dependent upon the conditions at the plate boundaries and upon the number of axial halfwaves of the buckled form. Tests on plates in axial compression have shown that the waveforms adopted at the onset of buckling may undergo abrupt changes further into the post-buckling regimes. Associated with these abrupt changes in waveform will be corresponding changes in axial stiffness. When loading is continued above the critical value there is, besides the possible abrupt changes in longitudinal waveform, a gradual transformation of the transverse waveform characterized by a flattening of the central regions of the plate. This phenomenon with its associated redistribution of axial mid-surface stresses has given rise to "effective width" concepts and has been studied in some detail by Koiter [1]. The present paper is concerned with abrupt changes in waveform of plates after buckling. The theoretical results obtained are plotted not as load vs. corresponding deformation but as load vs. out-of-plane buckling deflection since the latter, though of less practical significance, illustrate the mechanism of the buckling process much more clearly.

2. THEORY—THE PLATE EQUATIONS

Let us consider the problem of a thin rectangular plate loaded in its plane as shown in Fig. 1 and which is simply-supported on all four edges in the conventional sense and which has further specified restrictions on the boundary displacements. The mode of support is such that there are no out-of-plane deflections at the boundaries, the loaded edges remain straight and the longitudinal edges are not allowed to wave in the plane of the plate. The latter condition applies to a single panel of a multi-panelled infinitely wide plate loaded in axial compression, the junctions of the panels being knife-edge supports. It is further assumed that there is no restraint against lateral expansion of the

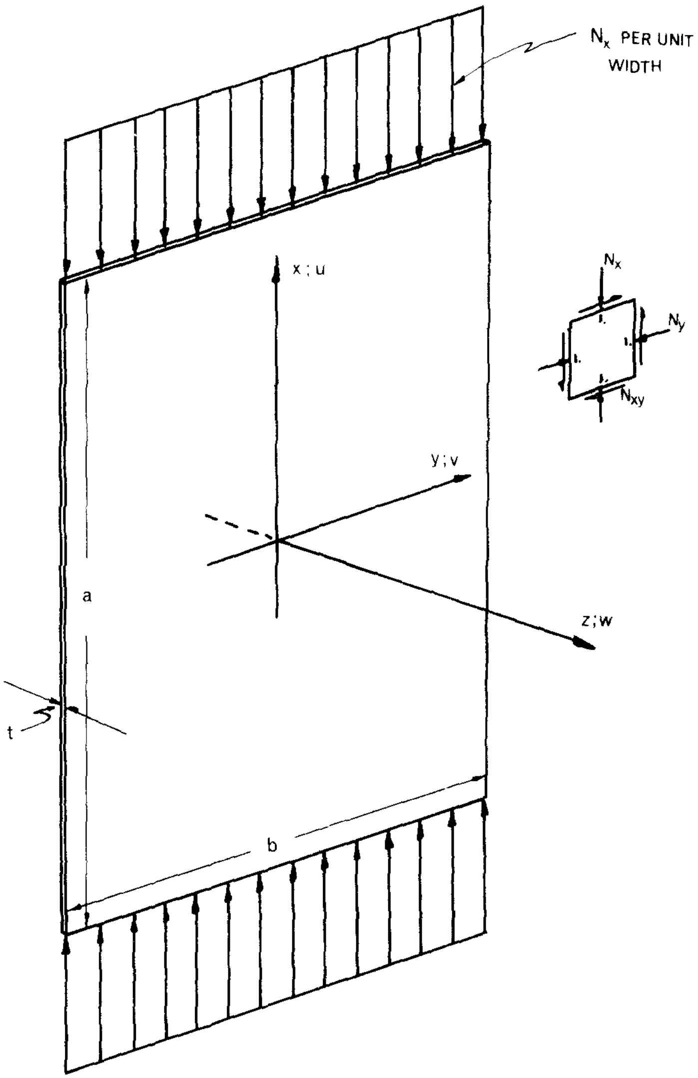

FIG. 1. Plate dimensions and definitions of symbols.

plate in its plane. Adopting the plate dimensions and co-ordinate axes as shown in Fig. 1 these boundary conditions may be written as

$$
\begin{aligned}
&\text{(i)} \quad (w)_{x=a/2;-a/2} = 0,\\
&\text{(ii)} \quad (w)_{y=b/2;-b/2} = 0,\\
&\text{(iii)} \quad (w_{,xx} + \nu w_{,yy})_{x=a/2;-a/2} = 0,\\
&\text{(iv)} \quad (w_{,yy} + \nu w_{,xx})_{y=b/2;-b/2} = 0,\\
&\text{(v)} \quad (u)_{x=a/2;-a/2} = \text{const.}\\
&\text{(vi)} \quad (v)_{y=b/2;-b/2} = \text{const.}
\end{aligned}
\tag{1}
$$

where a comma followed by subscripts represents partial differentiation in turn with respect to each subscripted variable. No restrictions are placed upon the other boundary displacements which will be discussed later together with results for other boundary conditions from different sources. The von-Kármán large deflection equations in the presence of initial geometric imperfections w^0 may be written in terms of w, w^0 and a stress function ϕ as follows

$$\begin{aligned} \nabla^4\phi &= E\{(w_{,xy})^2 - w_{,xx}w_{,yy} - [(w^0_{,xy})^2 - w^0_{,xx}w^0_{,yy}]\}, \\ \nabla^4(w-w^0) &= \frac{t}{D}\{\phi_{,yy}w_{,xx} - 2\phi_{,xy}w_{,xy} + \phi_{,xx}w_{,yy}\}, \end{aligned} \tag{2}$$

in which w represents the total out-of-plane deflection from the flat form and where ϕ is defined as

$$\phi_{,xx} = \frac{N_y}{t}; \qquad \phi_{,yy} = \frac{N_x}{t}; \qquad \phi_{,xy} = -\frac{N_{xy}}{t}. \tag{3}$$

An approximate solution of these equations is now obtained using a Ritz–Galerkin technique. We assume the following forms for w and w^0

$$\begin{aligned} w &= \cos\frac{\pi y}{b}\left(A\cos\frac{n\pi x}{a} + B\sin\frac{m\pi x}{a}\right), \\ w^0 &= \cos\frac{\pi y}{b}\left(A_0\cos\frac{n\pi x}{a} + B_0\sin\frac{m\pi x}{a}\right), \end{aligned} \tag{4}$$

satisfying boundary conditions (1)(i)–(iv). There is an apparent restriction on the evenness or oddness of m and n in (4) in order that boundary condition (1)(i) be satisfied; however, since the post-buckling equations (12) which result are interchangeable in $(n, \bar{A})$ and $(m, \bar{B})$ this restriction (which is merely a consequence of the selected position for the origin of the co-ordinate axes) becomes irrelevant. These expressions are substituted into the first of equations (2) (the compatibility equation) and the resulting equation solved for ϕ to give

$$\begin{aligned} \phi = &-\frac{E}{32}\left(A^2 - A_0^2\right)\left(\frac{a^2}{n^2b^2}\cos\frac{2n\pi x}{a} + \frac{n^2b^2}{a^2}\cos\frac{2\pi y}{b}\right) - \frac{Ea^2}{4b^2}\left(AB - A_0B_0\right)\left(\frac{1}{(m+n)^2}\right. \\ &\left.\times\sin\frac{(m+n)\pi x}{a} + \frac{1}{(m-n)^2}\sin\frac{(m-n)\pi x}{a}\right) - \frac{Ea^2b^2}{4}\cos\frac{2\pi y}{b}\left(AB - A_0B_0\right)\left(\alpha\sin\frac{(m+n)\pi x}{a}\right. \\ &\left.+\beta\sin\frac{(m-n)\pi x}{a}\right) + \frac{E}{32}\left(B^2 - B_0^2\right)\left(\frac{a^2}{m^2b^2}\cos\frac{2m\pi x}{a} + \frac{m^2b^2}{a^2}\cos\frac{2\pi y}{b}\right) - \frac{\lambda}{2bt}y^2, \end{aligned} \tag{5}$$

in which λ represents the total applied end load $\int_{-b/2}^{+b/2} N_x\,\mathrm{d}y$ and where α and β are defined as

$$\alpha = \frac{(m-n)^2}{\{(m+n)^2b^2 + 4a^2\}^2}, \qquad \beta = \frac{(m+n)^2}{\{(m-n)^2b^2 + 4a^2\}^2}. \tag{6}$$

The midsurface stresses may be derived from this expression for ϕ and thence by use of the strain–displacement relationships and the generalized Hooke's Law expressions may be obtained for u and v in terms of the midsurface stresses and w. When this is done it is found that u and v satisfy the boundary conditions (1)(v) and (vi) provided $(m+n)$ is an odd integer which will always be so for the cases considered herein. The variation of u along the longitudinal edges and the variation of v across the loaded edges may also be calculated from these expressions; it is assumed, however, that such movements may occur and are not restrained.

Next the expressions for w and ϕ are substituted into the second of equations (2) (the out-of-plane equilibrium equation) which will not be satisfied exactly but will have a residual R (say) owing to the approximate nature of w. The integral over the surface of the plate

$$\int_{-a/2}^{+a/2}\int_{-b/2}^{+b/2} Rw\,dx\,dy \tag{7}$$

has the dimensions of work and we define this as the excess energy of the plate. The Ritz–Galerkin approximation requires this virtual excess energy to vanish which leads to the two simultaneous equations

$$\begin{aligned}\int_{-a/2}^{+a/2}\int_{-b/2}^{+b/2} R\cos\frac{n\pi x}{a}\cos\frac{\pi y}{b}\,dx\,dy &= 0,\\ \int_{-a/2}^{+a/2}\int_{-b/2}^{+b/2} R\sin\frac{m\pi x}{a}\cos\frac{\pi y}{b}\,dx\,dy &= 0,\end{aligned} \tag{8}$$

which are non-linear algebraic equations in A, B, A_0 and B_0. Performing the substitutions and integrations equations (8) appear as

$$\begin{aligned}&\frac{3(1-\nu^2)a^2b^2}{16n^2}\left[\left(\frac{n^4}{a^4}+\frac{1}{b^4}\right)\left(\bar{A}^2-\bar{A}_0^2\right)+\frac{m^2n^2}{a^4}\left(\bar{B}^2-\bar{B}_0^2\right)\right]\bar{A}+12(1-\nu^2)\frac{a^2b^2}{n^2}\left(K-\frac{m^2n^2}{64a^4}\right)\\ &\qquad\times\left(\bar{A}\bar{B}-\bar{A}_0\bar{B}_0\right)\bar{B}+\frac{a^2b^2}{4n^2}\left(\frac{n^2}{a^2}+\frac{1}{b^2}\right)^2\left(\bar{A}-\bar{A}_0\right)-\frac{\lambda b}{4\pi^2D}\bar{A}=0,\\ &\frac{3(1-\nu^2)a^2b^2}{16m^2}\left[\left(\frac{m^4}{a^4}+\frac{1}{b^4}\right)\left(\bar{B}^2-\bar{B}_0^2\right)+\frac{m^2n^2}{a^4}\left(\bar{A}^2-\bar{A}_0^2\right)\right]\bar{B}+12(1-\nu^2)\frac{a^2b^2}{m^2}\left(K-\frac{m^2n^2}{64a^4}\right)\\ &\qquad\times\left(\bar{A}\bar{B}-\bar{A}_0\bar{B}_0\right)\bar{A}+\frac{a^2b^2}{4m^2}\left(\frac{m^2}{a^2}+\frac{1}{b^2}\right)^2\left(\bar{B}-\bar{B}_0\right)-\frac{\lambda b}{4\pi^2D}\bar{B}=0,\end{aligned} \tag{9}$$

where

$$K=\frac{1}{16b^4}+\frac{1}{64}[(m-n)^2\alpha+(m+n)^2\beta]+\frac{m^2n^2}{64a^4}, \tag{10}$$

and where

$$\bar{A}=\left(\frac{A}{t}\right),\quad \bar{B}=\left(\frac{B}{t}\right),\quad \bar{A}_0=\left(\frac{A_0}{t}\right),\quad \bar{B}_0=\left(\frac{B_0}{t}\right). \tag{11}$$

If we define an uncoupled buckling mode as a solution of equations (9) which involves only one of the deformation parameters $\bar{A}$ or $\bar{B}$, and a coupled buckling mode as a solution which involves both $\bar{A}$ and $\bar{B}$ then we might make the following observations:

(i) when $\bar{A}_0 = \bar{B}_0 = 0$; there are three solutions of equations (9), two are uncoupled the third coupled;
(ii) when $\bar{A}_0 \neq 0$, $\bar{B}_0 = 0$ or $\bar{A}_0 = 0$, $\bar{B}_0 \neq 0$; there are two solutions of equations (9), one is uncoupled the other coupled;
(iii) when $\bar{A}_0 \neq 0$, $\bar{B}_0 \neq 0$; there is one solution of equations (9) and this is coupled.

As is well-known the uncoupled buckling modes for the ideal plate are symmetric in character when plotted in the λ vs. A, B planes. Supple [2, 3] has made a detailed study in general terms of the possible forms of the coupled buckling modes for structural systems with two degrees of freedom which have symmetric uncoupled modes. Constant reference will be made to these works in the sequel. If we denote the uncoupled mode with the lower critical load as the primary mode and that with the higher critical load as the secondary mode then the results of Ref. [2] may be summarized using the notation of the present report as follows. The form of the $\bar{A}$ vs. $\bar{B}$ relationship of the coupled mode for perfect symmetrical structural systems, when real, may be either

(i) An ellipse; implying a transition path from the primary to the secondary mode.
(ii) A hyperbola branching from the primary mode; implying a further instability phenomenon after initial buckling.
(iii) A hyperbola branching from the secondary mode; implying that if the initial post-buckling is stable it will remain so.

It was shown in [3] that initial imperfections have an important and marked effect upon the post-buckling behaviour of systems in category (iii) above. These results have a direct relevance to the plate buckling equations (9).

3. THE IDEAL PLATE

In the absence of initial imperfections equations (9) reduce to

$$\begin{aligned} \bar{A}\left\{12(1-\nu^2)\frac{a^2b^2}{n^2}\left[\frac{1}{64}\left(\frac{n^4}{a^4}+\frac{1}{b^4}\right)\bar{A}^2+K\bar{B}^2\right]+\frac{a^2b^2}{4n^2}\left(\frac{n^2}{a^2}+\frac{1}{b^2}\right)^2-\frac{\lambda b}{4\pi^2 D}\right\} &= 0, \\ \bar{B}\left\{12(1-\nu^2)\frac{a^2b^2}{m^2}\left[\frac{1}{64}\left(\frac{m^4}{a^4}+\frac{1}{b^4}\right)\bar{B}^2+K\bar{A}^2\right]+\frac{a^2b^2}{4m^2}\left(\frac{m^2}{a^2}+\frac{1}{b^2}\right)^2-\frac{\lambda b}{4\pi^2 D}\right\} &= 0, \end{aligned} \tag{12}$$

from which the uncoupled buckling modes may be derived as

$$\begin{aligned} \frac{\lambda b}{4\pi^2 D} &= \frac{a^2b^2}{4n^2}\left(\frac{n^2}{a^2}+\frac{1}{b^2}\right)^2+\frac{12(1-\nu^2)}{64n^2}a^2b^2\left(\frac{n^4}{a^4}+\frac{1}{b^4}\right)\bar{A}^2, \\ \frac{\lambda b}{4\pi^2 D} &= \frac{a^2b^2}{4m^2}\left(\frac{m^2}{a^2}+\frac{1}{b^2}\right)^2+\frac{12(1-\nu^2)}{64m^2}a^2b^2\left(\frac{m^4}{a^4}+\frac{1}{b^4}\right)\bar{B}^2, \end{aligned} \tag{13}$$

and the $\bar{A}$–$\bar{B}$ relationship for the coupled buckling mode as

$$\left\{\frac{1}{64n^2}\left(\frac{n^4}{a^4}+\frac{1}{b^4}\right)-\frac{K}{m^2}\right\}\bar{A}^2+\left\{\frac{K}{n^2}-\frac{1}{64m^2}\left(\frac{m^4}{a^4}+\frac{1}{b^4}\right)\right\}\bar{B}^2 = \frac{1}{48(1-\nu^2)}\left\{\frac{1}{m^2}\left(\frac{m^2}{a^2}+\frac{1}{b^2}\right)^2 - \frac{1}{n^2}\left(\frac{n^2}{a^2}+\frac{1}{b^2}\right)^2\right\}. \tag{14}$$

If the plate aspect ratio is $\gamma = a/b$ and $m > n$ then if $\gamma^2 < mn$ the uncoupled mode with n half-waves is the primary mode and if $\gamma^2 > mn$ the uncoupled mode with m half-waves is the primary mode. The right-hand side of equation (14) is negative when $\gamma^2 > mn$ and positive when $\gamma^2 < mn$. The coefficient of $\bar{A}^2$ is always negative and the coefficient of $\bar{B}^2$ always positive. As a result the form of equation (14) is a hyperbola and the coupled mode always branches from the secondary mode. For loads greater than that at which the coupled mode branches from the secondary mode the latter is stable [4].

The post-buckling equilibrium paths for an ideal plate with $\gamma = 2, m = 3, n = 2$, $\nu = \frac{1}{3}$ are shown in Fig. 2. It may be noted that in equations (13) $(4\pi^2 D)/b$ is the classical

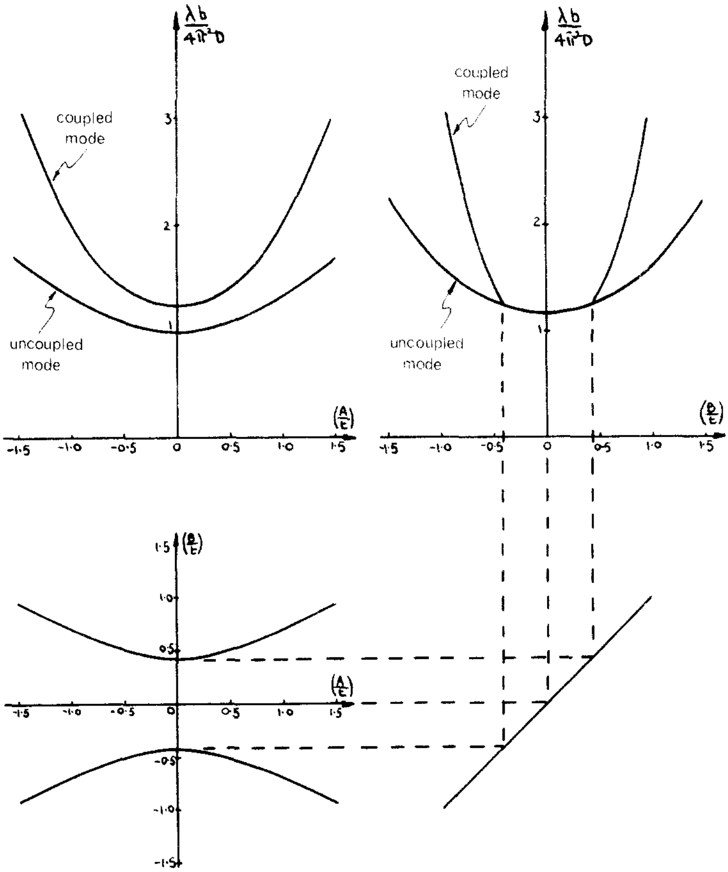

FIG. 2. Post-buckling equilibrium paths for a simply-supported plate $\gamma = 2$, $m = 3$, $n = 2$, $\nu = \frac{1}{3}$ with edges held straight.

buckling load of a simply-supported plate whose aspect ratio is an integer and accordingly the first terms on the right-hand sides represent the buckling stress coefficient (normally referred to in the texts as k_c) divided by four. We may calculate the critical loads at which the coupled mode bifurcates from the secondary mode and thus define what we might term the *coupled buckling stress coefficient* ${}^c k_c$ related to the buckling stress coefficient as follows:

$$
{}^{c}k_c = k_c + \left\{ \frac{\left(\dfrac{n^2b^2}{a^2} + \dfrac{a^2}{n^2b^2}\right)\left[\dfrac{1}{m^2}\left(\dfrac{m^2}{a^2} + \dfrac{1}{b^2}\right)^2 + \dfrac{1}{n^2}\left(\dfrac{n^2}{a^2} + \dfrac{1}{b^2}\right)^2\right]}{\dfrac{1}{n^2}\left(\dfrac{n^4}{a^4} + \dfrac{1}{b^4}\right) - \dfrac{64K}{m^2}} \right\}. \tag{15}
$$

This inter-relationship is illustrated in Fig. 3 for varying aspect ratios: the values of ${}^{c}k_c$ are shown by the dash-dot curves. It can be seen that as γ increases the critical loads for buckling in the uncoupled and coupled modes rapidly converge.

4. INITIAL IMPERFECTIONS

If, for convenience, we consider that buckling in n halfwaves longitudinally represents the primary buckling mode for a plate then we may divide the buckling of imperfect plates into three classes. These are:—

(i) imperfections in primary mode, $\bar{A}_0 \neq 0, \bar{B}_0 = 0$, .

(ii) imperfection in secondary mode, $\bar{A}_0 = 0, \bar{B}_0 \neq 0$, (16)

(iii) imperfections in both modes, $\bar{A}_0 \neq 0, \bar{B}_0 \neq 0$.

From the general theory of Ref. [3] we know that when there is only an initial imperfection in the form of the primary mode then the plate will deform into this mode and no interaction from the secondary mode occurs. For example, if we prescribe $m = 3, n = 2, \nu = \frac{1}{3}$ and $\bar{B}_0 = 0$ then the first of equations (9) becomes

$$
0{\cdot}333\bar{A}(\bar{A}^2 - \bar{A}_0^2) + 1{\cdot}395\bar{A}\bar{B}^2 + (\bar{A} - \bar{A}_0) - \frac{\lambda b}{4\pi^2 D}\bar{A} = 0 \tag{17}
$$

and the $\bar{A}$–$\bar{B}$ relationship of the coupled mode is

$$
2{\cdot}50\bar{A}_0 + 0{\cdot}434\bar{A} + 0{\cdot}416\bar{A}\bar{A}_0^2 - 2{\cdot}375\bar{A}\bar{B}^2 + 0{\cdot}719\bar{A}^3 = 0. \tag{18}
$$

Figure 4 shows the post-buckling equilibrium paths obtained from equations (17) and (18) when $\bar{A}_0 = 1{\cdot}0$; the equilibrium paths for the perfect plate are shown as broken lines. Besides the natural loading path, which the plate follows when loaded, all the complementary paths are shown for the sake of completeness.

When only an initial imperfection in the form of the secondary mode is present i.e. $\bar{A}_0 = 0$ then with $m = 3, n = 2, \nu = \frac{1}{3}$ the first of equations (9) reduces to the form

$$
0{\cdot}333\bar{A}^2 + 1{\cdot}395\bar{B}^2 - 0{\cdot}375\bar{B}_0^2 + 1{\cdot}00 - \frac{\lambda b}{4\pi^2 D} = 0, \tag{19}
$$

and the $\bar{A}$–$\bar{B}$ relationship of the coupled mode is now

$$
2{\cdot}94\bar{B}_0 - 0{\cdot}434\bar{B} - 0{\cdot}72\bar{A}^2\bar{B} + 0{\cdot}185\bar{B}\bar{B}_0^2 + 2{\cdot}37\bar{B}^3 = 0. \tag{20}
$$

When $\bar{A} = 0$ equation (20) may have one or three real roots for $\bar{B}$ depending on the magnitude of the imperfection $\bar{B}_0$. That value of $\bar{B}_0$ that makes two of the roots real and equal represents a critical imperfection [3] and from equation (20) this value for the assumed

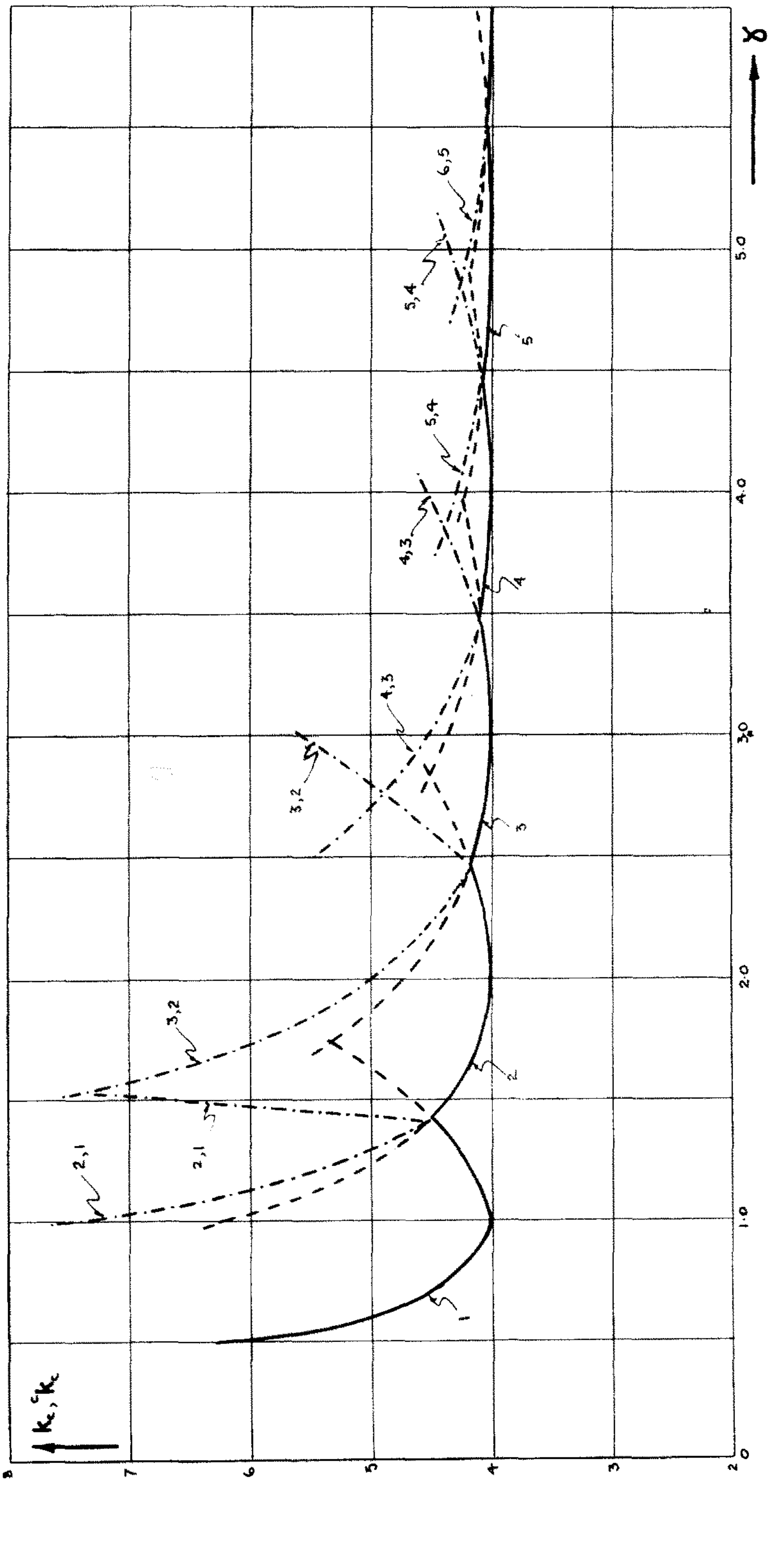

FIG. 3. Critical loads for coupled and uncoupled modes of buckling.

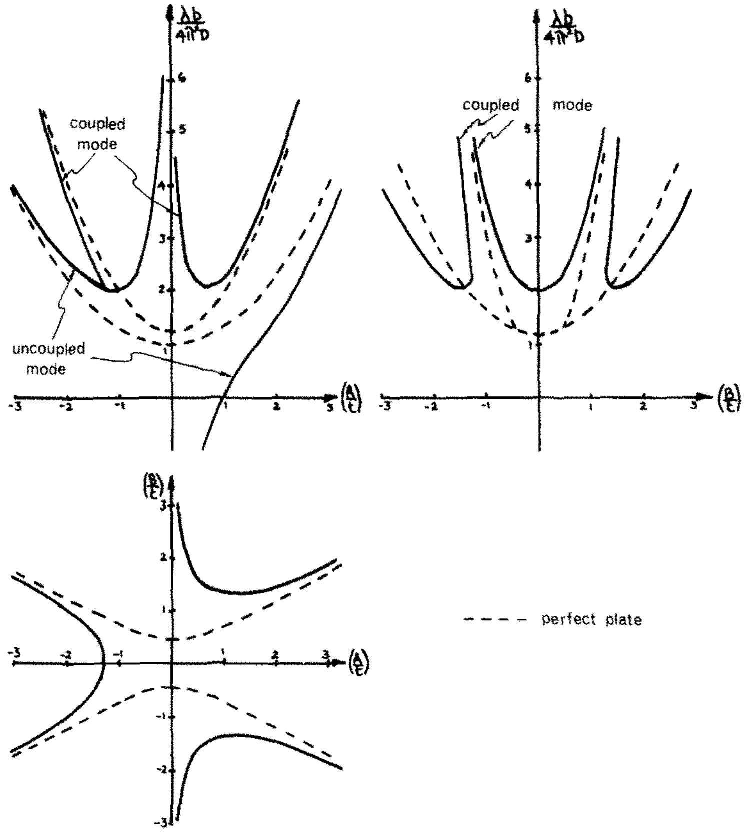

FIG. 4. Post-buckling equilibrium paths for imperfect plate $\gamma = 2$, $m = 3$, $n = 2$, $\nu = \frac{1}{3}$ with initial imperfection $\bar{A}_0 = 1{\cdot}0$.

magnitudes of γ, ν, m, n is

$$(\bar{B}_0)_{\text{crit}} = 0{\cdot}025. \tag{21}$$

If $\bar{B}_0 > (\bar{B}_0)_{\text{crit}}$ the buckled form of the plate develops as three halfsinewaves and there is no interaction from the primary two-halfwave mode. If $B_0 < (B_0)_{\text{crit}}$ the plate initially develops in the three-halfsinewave mode but this mode then becomes unstable at a point of bifurcation whereupon the plate buckles into a coupled mode which on further loading approaches asymptotically to the primary two-halfsinewave mode. These points are illustrated in Figs. 5 and 6; in Fig. 5 the initial imperfection $\bar{B}_0 = 0{\cdot}020$ and in Fig. 6 $\bar{B}_0 = 1{\cdot}00$.

Finally, when both initial imperfections $\bar{A}_0$ and $\bar{B}_0$ are non-zero the buckling equations for the arbitrarily assigned values $m = 3$, $n = 2$, $\nu = \frac{1}{3}$ appear as

$$A - A_0 + 0{\cdot}333(\bar{A}^2 - \bar{A}_0)\bar{A} + 0{\cdot}375(\bar{B}^2 - \bar{B}_0^2)\bar{A} + 1{\cdot}02(\bar{A}\bar{B} - \bar{A}_0\bar{B}_0)\bar{B} - \frac{\lambda b}{4\pi^2 D}\bar{A} = 0,$$

$$0{\cdot}294\bar{A}\bar{B}_0 - 0{\cdot}25\bar{B}\bar{A}_0 - 0{\cdot}434\bar{A}\bar{B} - 0{\cdot}071\bar{A}^3\bar{B} + 0{\cdot}237\bar{A}\bar{B}^3 + 0{\cdot}0185\bar{A}\bar{B}\bar{B}_0^2 - 0{\cdot}0416\bar{A}\bar{B}\bar{A}_0^2$$
$$+ 0{\cdot}112\bar{A}^2\bar{A}_0\bar{B}_0 - 0{\cdot}255\bar{B}^2\bar{B}_0\bar{A}_0 = 0. \tag{22}$$

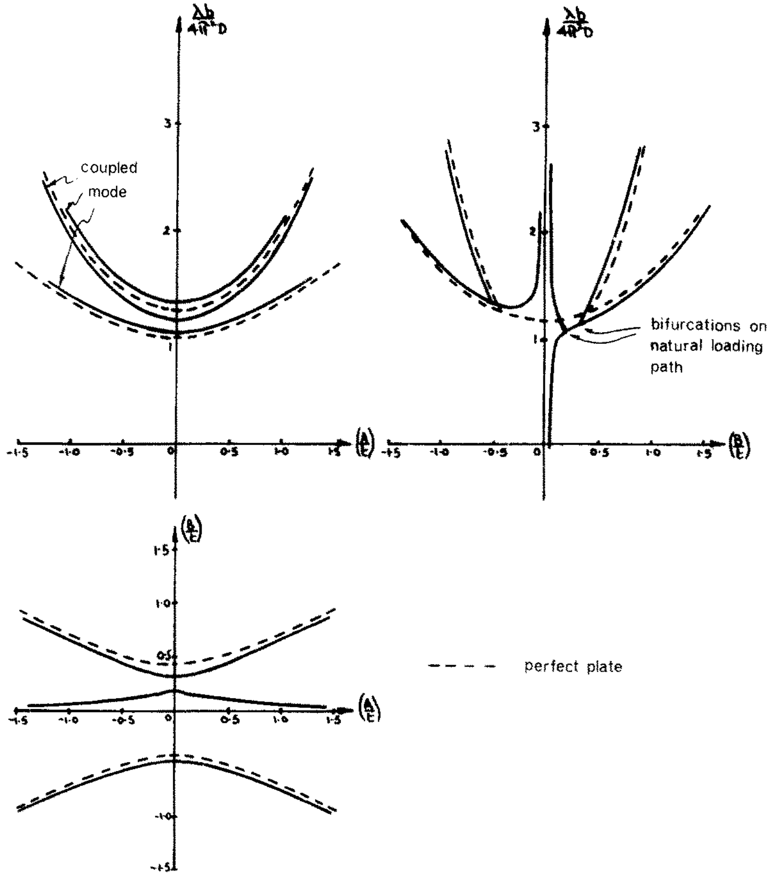

FIG. 5. Post-buckling equilibrium paths for imperfect plate $\gamma = 2$, $m = 3$, $n = 2$, $\nu = \frac{1}{3}$ with initial imperfection $\bar{B}_0 = 0{\cdot}020$.

The forms of the solution to these equations are shown in Fig. 7 for two combinations of initial imperfections $\bar{A}_0$ and $\bar{B}_0$. It is clear from the results shown that for a given value of $\bar{A}_0$ there is a critical value of $\bar{B}_0$ for which the stability of the natural loading path is lost at a point of bifurcation; when $\bar{A}_0 = 0$ this corresponds to the critical value of $\bar{B}_0$ already discussed. By ignoring second order terms of $\bar{A}_0$ and $\bar{B}_0$ in equations (9) we may derive the approximate locus of critical imperfections (i.e. combinations of $\bar{A}_0$ and $\bar{B}_0$ which produce a branching solution on the natural loading path) in the form [3]

$$K_1 \bar{A}_0^{\frac{2}{3}} + K_2 \bar{B}_0^{\frac{2}{3}} = K_3, \tag{23}$$

where

$$K_1 = \left\{12(1-\nu^2)\left[\frac{1}{64n^2b^4} - \frac{K}{m^2} + \frac{n^2}{64a^4}\right]\right\}^{\frac{1}{3}} \left\{\frac{1}{8n^2}\left(\frac{n^2}{a^2} + \frac{1}{b^2}\right)^2\right\}^{\frac{2}{3}},$$

$$K_2 = \left\{12(1-\nu^2)\left[\frac{K}{n^2} - \frac{1}{64m^2b^4} - \frac{m^2}{64a^4}\right]\right\}^{\frac{1}{3}} \left\{\frac{1}{8m^2}\left(\frac{m^2}{a^2} + \frac{1}{b^2}\right)^2\right\}^{\frac{2}{3}},$$

$$K_3 = \frac{(m^2-n^2)}{12m^2n^2}\left(\frac{m^2n^2}{a^4} - \frac{1}{b^4}\right). \tag{24}$$

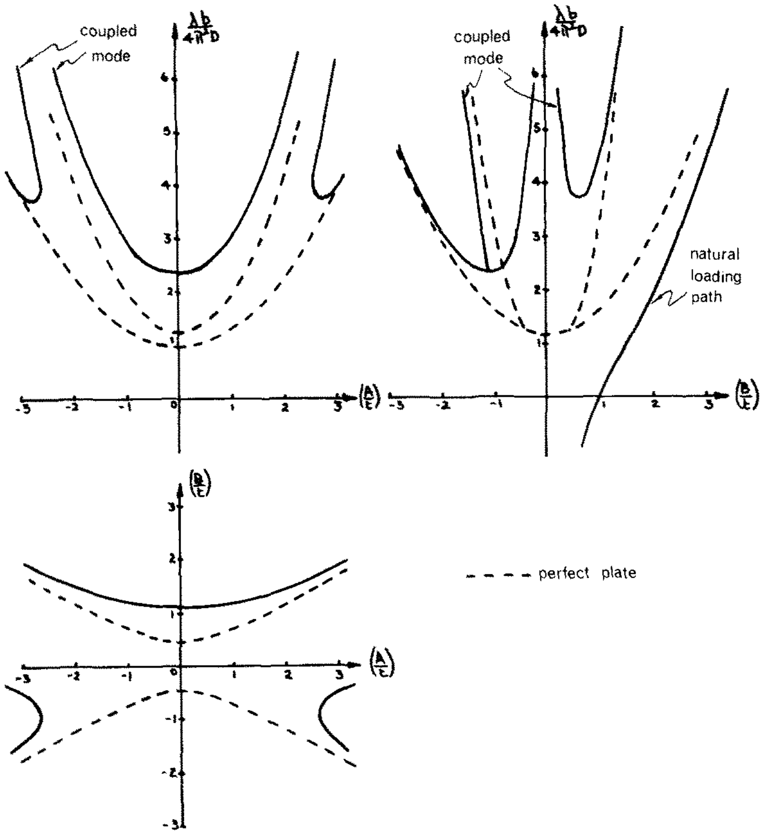

FIG. 6. Post-buckling equilibrium paths for imperfect plate $\gamma = 2$, $m = 3$, $n = 2$, $\nu = \frac{1}{3}$ with initial imperfection $B_0 = 1{\cdot}0$.

This critical locus is shown plotted in Fig. 7 for the appropriate values of γ, m, n, ν and divides the set of positive initial imperfections $(\bar{A}_0, \bar{B}_0)$ into two sub-sets. If the initial imperfection belongs to the sub-set containing the $\bar{A}_0$ axis then at loads of approximately twice the classical buckling load the buckling mode is predominantly two halfsinewaves; if the initial imperfection belongs to the other sub-set then at these loads the buckling mode is predominantly three halfsinewaves. It might be emphasized again that in the absence of initial imperfections buckling would be in a purely two-halfsinewave mode.

5. OTHER BOUNDARY CONDITIONS

The behaviour after buckling of plates in compression is dependent upon the conditions prevailing at the boundaries. If the plates are treated as systems with two degrees of freedom and are isotropic and un-reinforced then the uncoupled buckling modes will be symmetric in character and the coupled mode will belong to one of the categories given in Ref. [2] and summarized in Section 2 of the present paper. It has been shown by Hlavacek [5] that for a simply-supported plate which is allowed to expand laterally and whose unloaded edges are free to wave in the plane of the plate the coupled buckling mode is of

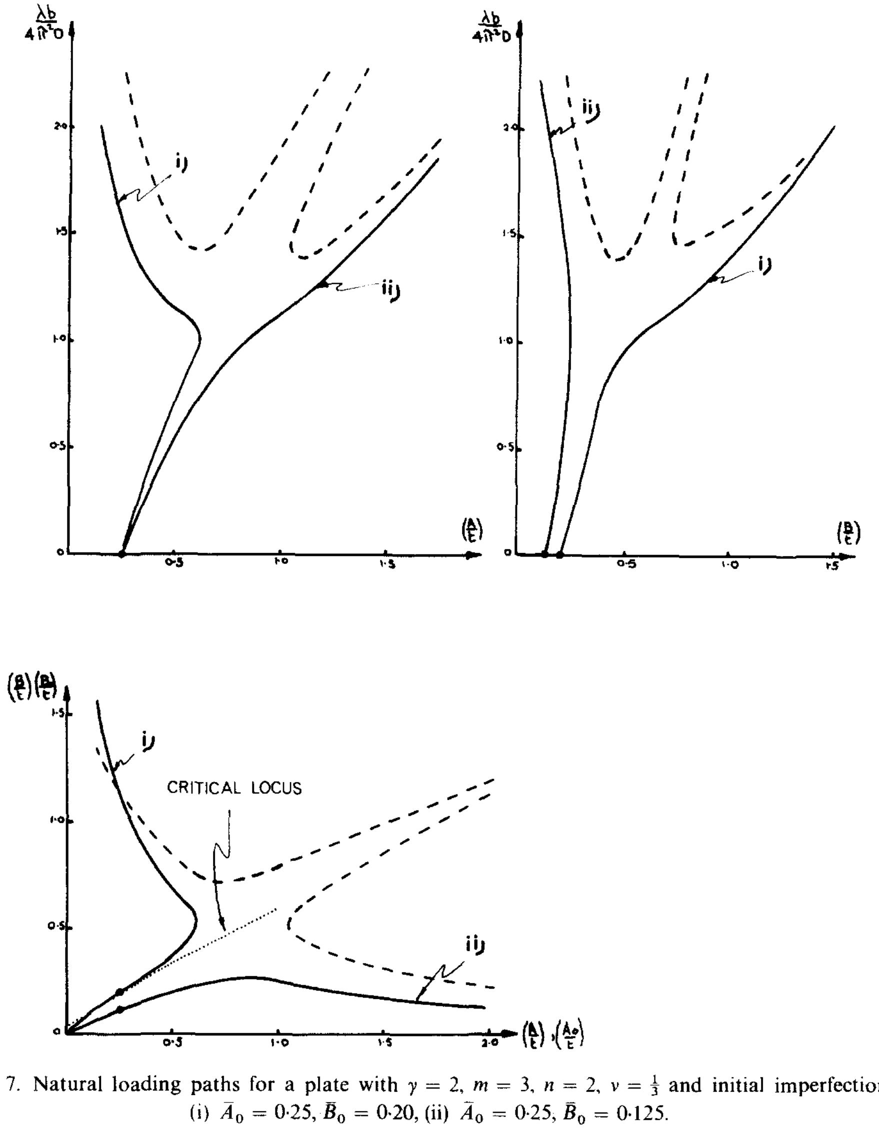

FIG. 7. Natural loading paths for a plate with $\gamma = 2$, $m = 3$, $n = 2$, $\nu = \frac{1}{3}$ and initial imperfections (i) $\bar{A}_0 = 0{\cdot}25$, $\bar{B}_0 = 0{\cdot}20$, (ii) $\bar{A}_0 = 0{\cdot}25$, $\bar{B}_0 = 0{\cdot}125$.

the hyperbola type branching from the upper uncoupled buckling mode. Again, Supple [4] has shown the same type of coupling behaviour to exist for the simply-supported plate which is free to expand laterally and whose unloaded edges are clamped. Therefore, for these two types of boundary conditions the post-buckling behaviour of plates is qualitatively the same as that described in Section 2 of the present paper. Major changes [6] in waveform after initial buckling for these boundary conditions would be explained by the presence of initial imperfections.

If the plate is restrained from expanding laterally then the form of the coupled buckling mode is dependent upon the value of Poissons ratio of the plate material. This observation follows from the results of Sharman and Humpherson [7] who analysed the buckling behaviour of a simply-supported plate whose unloaded edges are rigidly held apart. In the terminology of the present report the buckling equations corresponding to equations (9) obtained by these authors appear in the forms

$$\bar{B}\left\{12(1-\nu^2)\left[\left(\frac{1+3\gamma^4}{16}\right)\bar{B}^2+Q_1\bar{A}^2\right]+(1+\gamma^2)^2-\frac{\lambda a^2}{\pi^2 Db}(1+\gamma^2\nu)\right\} = 0,$$
$$\bar{A}\left\{12(1-\nu^2)\left[\left(\frac{16+3\gamma^4}{16}\right)\bar{A}^2+Q_1\bar{B}^2\right]+(4+\gamma^2)^2-\frac{\lambda a^2}{\pi^2 Db}(4+\gamma^2\nu)\right\} = 0, \quad (25)$$

where

$$Q_1 = \tfrac{1}{8}(2+3\gamma^4)+\frac{81\gamma^4}{16(1+4\gamma^2)^2}+\frac{\gamma^4}{16(9+4\gamma^2)^2}, \quad (26)$$

and where buckling in two and one halfsinewaves only have been considered corresponding to $\bar{A}$ and $\bar{B}$ respectively. The $\bar{A}$–$\bar{B}$ relationship for the coupled mode follows from equations (25) in the form

$$\left\{Q_1(4+\gamma^2\nu)-\frac{(16+3\gamma^4)}{16}(1+\gamma^2\nu)\right\}\bar{A}^2+\left\{\frac{(1+3\gamma^4)}{16}(4+\gamma^2\nu)-Q_1(1+\gamma^2\nu)\right\}\bar{B}^2$$
$$= \frac{(4-\gamma^4+5\gamma^2\nu+2\gamma^4\nu)}{4(1-\nu^2)}, \quad (27)$$

which when real represents an ellipse or hyperbola as anticipated. The results for the forms of the coupled buckling mode derived from equation (27) are summarized in Fig. 8 which is a plot of aspect ratio γ against Poissons ratio ν. The unbroken curve represents simultaneous buckling i.e. the values of γ and ν at which the critical loads for buckling

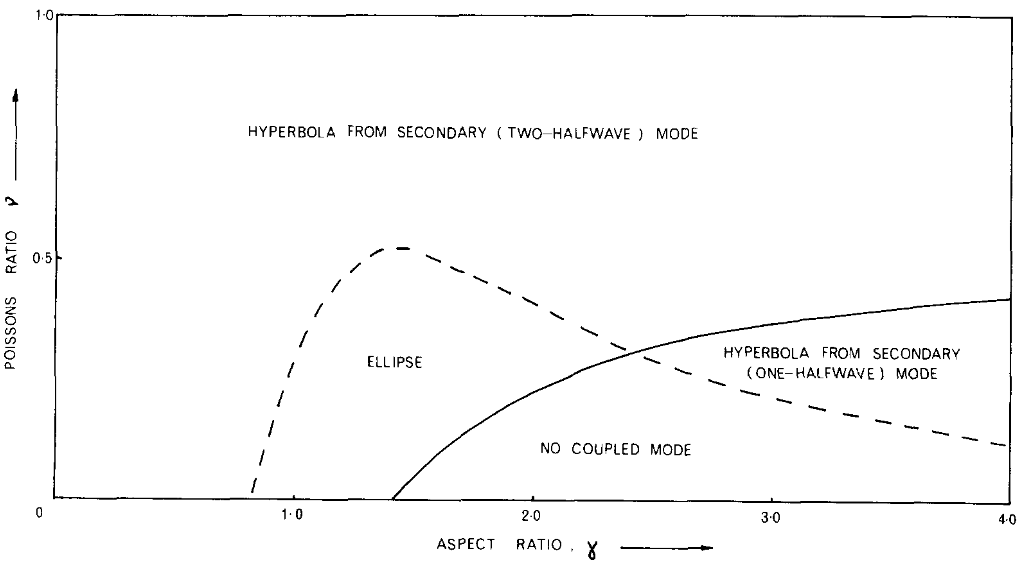

FIG. 8. Forms of coupled buckling mode for a simply-supported plate with longitudinal edges rigidly held apart for $m = 1$, $n = 2$.

in one and two halfsinewaves are equal, this condition being given by the equation

$$4-\gamma^4+5\gamma^2\nu+2\gamma^4\nu = 0. \tag{28}$$

The lower right portion of the figure represents values of γ and ν for which buckling in two halfsinewaves is the primary mode. It may be noted that equation (28) is the same as the right-hand side of equation (27) indicating that there is a modification of the form of the coupled mode when the branching points of the uncoupled modes coalesce [2]. Any change in sign of the coefficients of $\bar{A}^2$ or $\bar{B}^2$ in equation (27) also represents a change in form of the coupling solution. The broken curve in Fig. 8 represents the values of γ and ν at which the coefficient of $\bar{B}^2$ in equation (27) becomes equal to zero; the coefficient of $\bar{A}^2$ maintains the same sign for all positive values of γ and ν.

As an example we may consider the plate with aspect ratio 2 and Poissons ratio $\frac{1}{3}$. We see that the lowest critical load is associated with buckling in one halfsinewave which is thus the primary mode, and that the coupled mode is of the ellipse type. The load–deformation characteristics for this case are illustrated in Fig. 9; it is seen that the plate initially buckles in one halfsinewave and then snaps to the two halfsinewave form at a

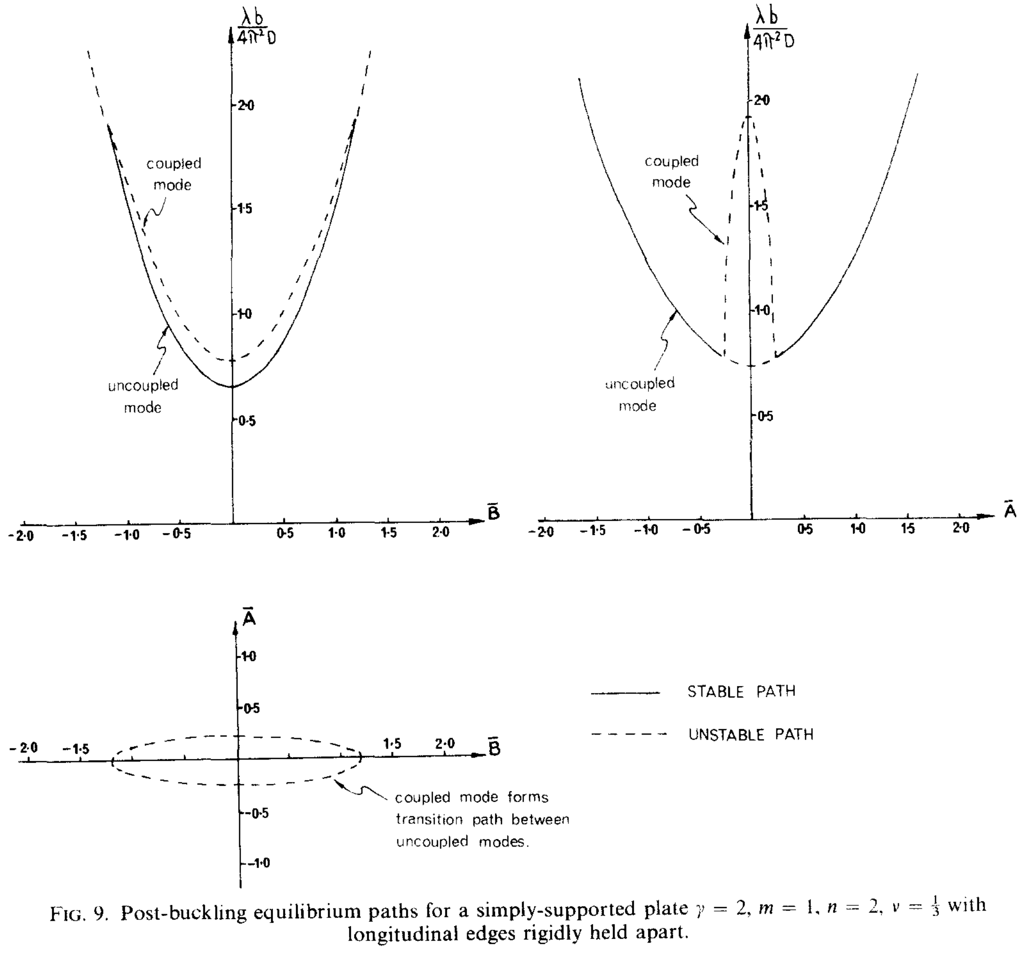

FIG. 9. Post-buckling equilibrium paths for a simply-supported plate $\gamma = 2$, $m = 1$, $n = 2$, $\nu = \frac{1}{3}$ with longitudinal edges rigidly held apart.

load which is approximately 2·8 times the initial buckling value. With these boundary conditions, therefore, it is possible for the *ideal* plate to undergo a change in buckle pattern provided the load mentioned is attained. Any initial imperfection with a two halfsinewave component would tend to reduce the load value at which the plate snaps from a predominantly one halfsinewave form to a predominantly two halfsinewave form.

The effect of lateral pressures on a plate in axial compression is very similar to that of initial geometric imperfections. A uniform pressure would tend to induce buckling in

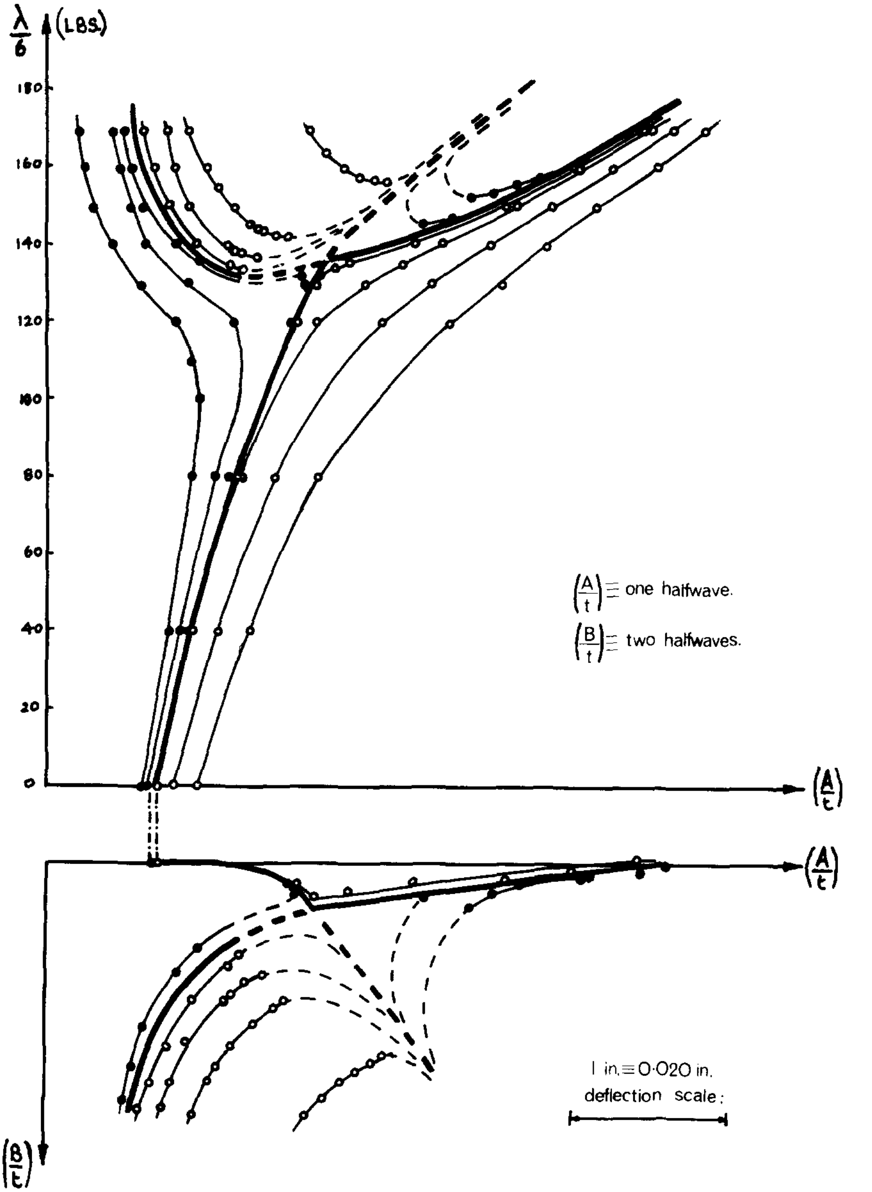

FIG. 10. Experimental load–buckling deflection curves for a simply-supported plate with longitudinal edges free to wave in the plane of the plate with $\gamma = 2$, $t = 0{\cdot}030$ in. and varying initial imperfections.

one halfsinewave and therefore with boundary conditions (1) would produce similar behaviour to an initial imperfection in the primary mode for $\gamma < \sqrt{2}$ and similar behaviour to an initial imperfection in a secondary mode for $\gamma > \sqrt{2}$, [4]. If the pressure were linearly varying in the axial direction [7] then it would produce a similar effect to an initial geometric imperfection with components in one and two halfwaves.

Tests have been performed on simply-supported plates in axial compression [4] with boundary conditions the same as those given in the analysis by Hlavacek [5]. The initial imperfections in one and two halfwaves in a plate with aspect ratio $\gamma = 2$ were varied artificially by the application of small lateral point loads acting at the half and quarter points of the plate axis and the resulting load deflection behaviour studied for various combinations of induced initial imperfections. The experimental behaviour verified the form of post-buckling expected for a system with a hyperbolic coupled mode branching from the secondary uncoupled mode predicted theoretically by Hlavacek. Figure 10, which is reproduced from Ref. [4], shows the experimental load vs. buckling deflection curves for a plate of aspect ratio $\gamma = 2$, displaying coupling characteristics mainly in one and two halfwaves, for various combinations of induced initial imperfections.

6. CONCLUSION

From the results of the preceding sections it is apparent that the post-buckling behaviour of short plates can be quite complex. With the assumption that such plates may be treated as two-degrees-of-freedom systems it has been shown that the post-buckling behaviour especially with regard to change in buckle pattern is dependent upon the prevailing boundary conditions and the existence of initial geometric imperfections. A multi-mode analysis would almost certainly arrive at the same conclusions. It is hoped that the present two-mode analysis in conjunction with the results of two-mode analyses from other sources presented together in this paper go some way in clarifying the mechanism by which major changes in waveform of plates in the post-buckling regime are brought about.

REFERENCES

[1] W. T. KOITER, NLL Report S287, Amsterdam, December (1943).
[2] W. J. SUPPLE, *Int. J. Mech. Sci.* **9**, 97 (1967).
[3] W. J. SUPPLE, *Int. J. Mech. Sci.* **10**, 737 (1968).
[4] W. J. SUPPLE, Coupled buckling modes of structures. Thesis, London University (1966).
[5] I. HLAVACEK, *Acta Tech. CSAV Praha*, No. 2 (1962).
[6] W. J. SUPPLE and A. H. CHILVER, Elastic post-buckling of compressed rectangular flat plates. *Thin-Walled Structures*, edited by A. H. CHILVER. Chatto & Windus (1967).
[7] P. W. SHARMAN and J. G. HUMPHERSON, *Aero. J. R. Aero. Soc.* **72**, 431 (1968).

(*Received* 22 *September* 1969; *revised* 2 *February* 1970)

Абстракт—Обсуждается закритическое поведение прямоугольных пластинок, подверженных действию сжатия в осевом направлении. Рассматриваются пластинки, обладающие двумя степенями свободы, что характеризуется выпучиванием в осевом направлении *м* и *n* полусинусоидальными волнами. Несопряженные и сопряженные формы выпучивания даются для заданных граничных условий. Используются результаты исследований совместно с результатами полученными другими способами для разных граничных условий, в целью выяснения внезапных изменений формы волн, в пластинках в закритическом состоянию. Эффекты начальных геометрических неправильностеи рассматриваются в качестве необходимой части анализа.